Journal of the Research Institute of Basic Sciences,
Korea Maritime University, Vol. 4, 1994.

Fatigue Characteristics of a Two-phase Cast Stainless Steel

Yun Hae Kim

Department of Materials Engineering,
Korea Maritime University, Pusan, Korea

Introduction

At low $\triangle K$ levels the Paris law does not always hold and the threshold stress intensity for crack growth, $\triangle K_{th}$, is approach where the condition for crack growth is described by $\triangle K \geq \triangle K_{th}$ [1]. The crack propagation process in the near threshold region is considerably influenced by three distinct types of crack closure phenomena, described as plastic-, oxide- and fracture surface roughness induced crack closure.

It has been reported that the microstructure, stress ratio, R, and environment also have a significant effect on near threshold fatigue crack growth behavior [2]. In the present study, the effects of microstructure and fracture surface roughness on $\triangle K_{th}$ and the near threshold fatigue crack growth rate have been investigated for a two-phase cast stainless steel.

2. Materials and Experimental Procedure

The material used was a ferritic-austenitic, duplex, stainless steel having the chemical composition(wt%); C, 0.021; Si, 0.85; Mn, 0.98; P 0.009; S, 0.008; Ni, 6.01; Cr, 22.9; Mo, 3.01; N, 0.13. Heat treatment consisted of a solution treatment at $1353K$ for 4h followed by water cooling. The mechanical properties of as-cast specimens and heat-treated specimens are presented in Table 1. Microsuructures of the as-cast specimens and the heat-treated specimens are shown in Fig.1. Fatigue tests were carried out

using 14mm thick CT specimens, on an MTS electro-hydraulic fatigue testing machine. The measurement of crack closure was done using the unloading elastic compliance method and the load-displacement curve determined with a strain gauge fitted on the back surface of the specimen. The threshols, ΔK_{th}, was determined in terms of the ΔK at which no crack growth could

Table 1. Mechanical properties

	Tension test				Charpy absorbed energy (J)	
	σ_{ys} (MPa)	σ_{uts} (MPa)	El. (%)	BHN (H_B)	+20°C	−30°C
As-cast material	532	751	27.0	248	45.1	7.9
Heat-treated material	513	687	28.9	229	176.0	173.1

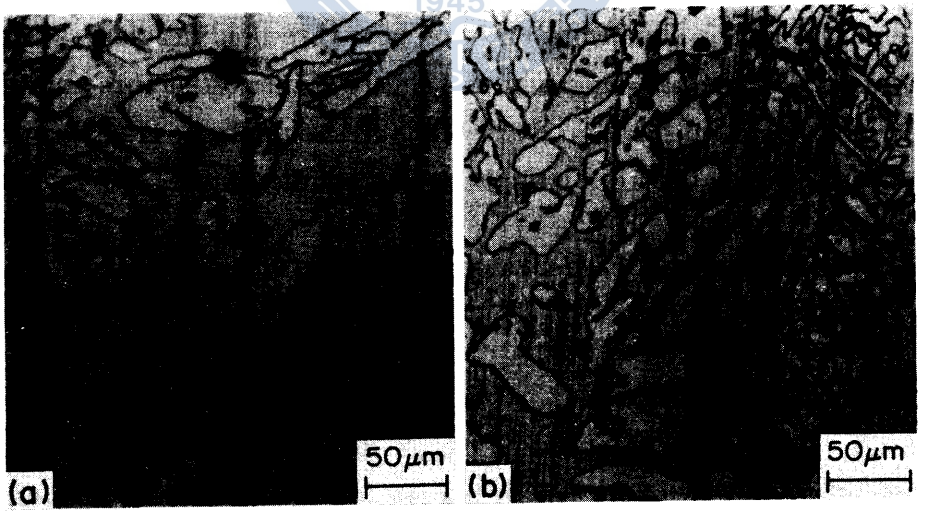

Fig. 1. Microstructures of as-cast and heat-treated specimens: (a) as-cast material; (b) heat-treated material.

be detected within 10^7 cycles. This corresponds to a threshold defined in terms of a maximum crack growth rate of less than $10^{-8} mm/cycle$. The loading conditions were given by stress ratios of $R = 0.12$ and 0.6 and a constant frequency of $20Hz$.

3. Experimental Result and Discussion

The fatigue crack growth rate for as-cast material and for heat-treated material at two stress ratios is illustrated in Fig.2 as a function of ΔK. As

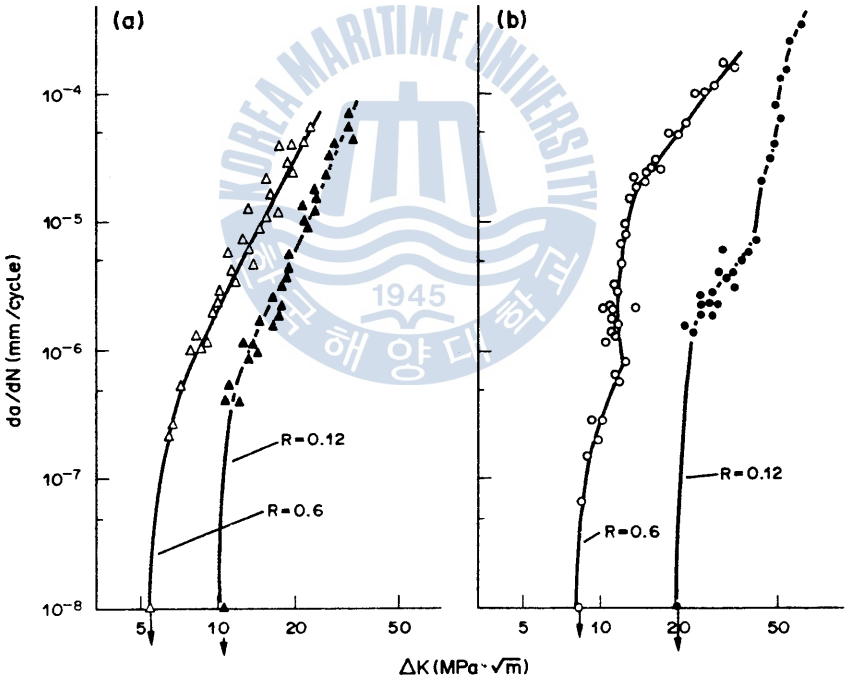

Fig. 2. Relationship between da/dN and ΔK at $R = 0.12$ and 0.6: (a) as-cast material; (b) heat-treated material.

the stress ratio increases, the crack growth rate also increases. This increases

in crack growth rate is similar for the heat-treated material. At high ΔK values the heat-terated material approaches that of the as-cast material. In the low ΔK range, the crack growth rate of the as-cast material is greater than that of the heat-terated material. Threshold data for both materials at a crack growth rate of $10^{-8} mm/cycle$ are given in Fig.2. The threshold for as-cast material decreases from10 to $5MPa\sqrt{m}$ as stress ratio increases from 0.12 to 0.6. The ΔK_{th} value is greater for the heat-treated material than for the as-cast material.

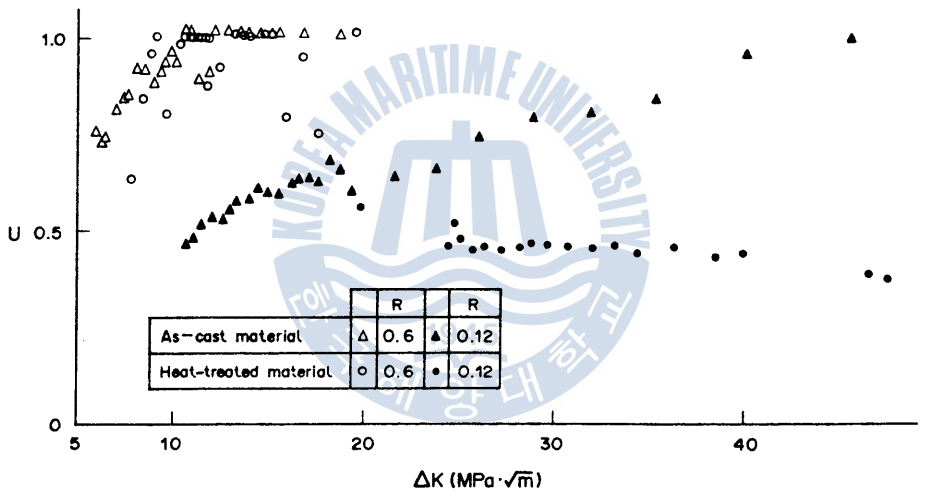

Fig. 3. Variation of U with ΔK.

The variation of crack opening ratio, U, with ΔK is shown in Fig.3, where the U value is defined by the ratio of crack opening stress intensity factor to maximum stress intensity factor. The crack opening ratio, U, is mostly lower for the heat-treated material than for as-cast material. At $R = 0.12$ there is increasing separation between the curves with increasing ΔK showing microstructure has a significant effect on the crack opening ratio, U. The crack growth rate for both materials is plotted aginst the

effective stress intensity factor, ΔK_{eff}, in Fig.4 at stress ratio of 0.12 and 0.6. It can be seen from Fig.4 that for the as-cast material the effect of stress

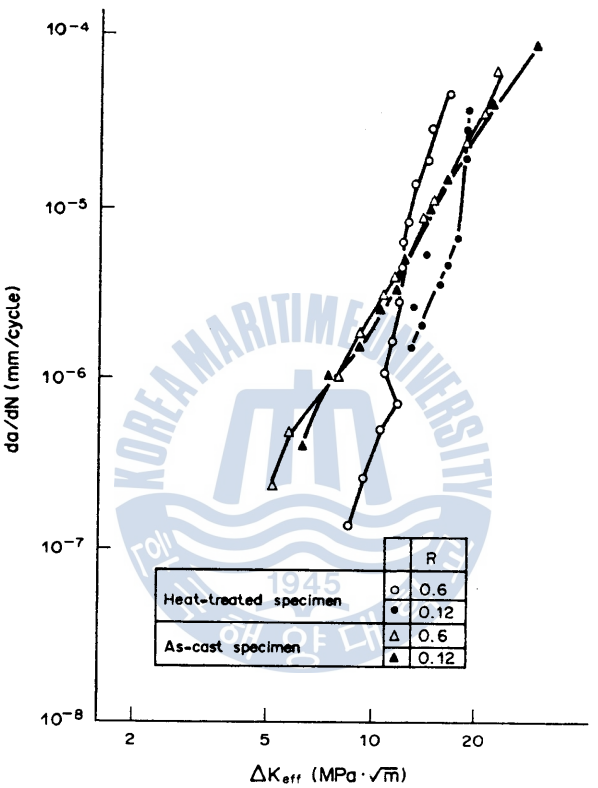

Fig. 4. Crack growth rate vs ΔK_{eff}.

ratio can be removed by the use of the effective stress intensity, ΔK_{eff}. The same is true for the heat-treated alloy at high ΔK_{eff} values where the data are close to that for the as-cast material. At lower ΔK_{eff} values, the separation between the two sets of data reflects microstructural effects.

The distribution of fracture surface roughness of an as-cast specimen

tested at $R = 0.6$ is shown in Fig.5 where H is the profile-height, a the crack

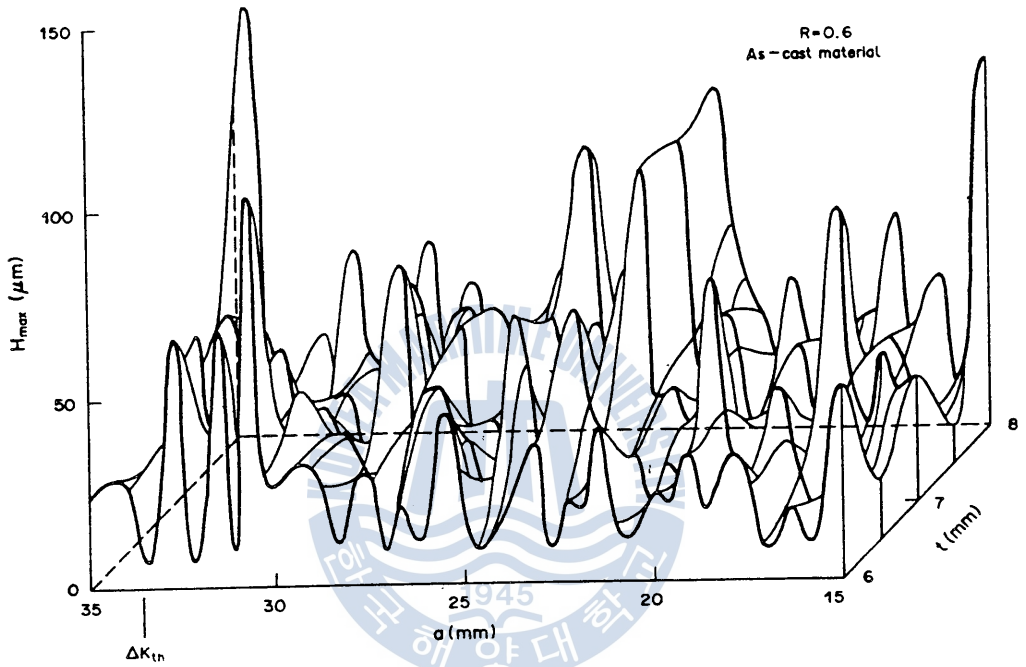

Fig. 5. Distribution of fracture surface roughness for an as-cast specimen at $R = 0.6$.

length and t the specimen thickness. It can be seen that the general fracture surface roughness is large. The fracture surface roughness for a heat-treated specimen at $R = 0.6$ and 0.12 is illustrated in Fig.6. It can be seen from Fig.5 and 6 that the fracture surface generally tends to be rougher for the as-cast material except between $a = 20$ and $25mm$.

It can be seen from Fig.1 that there is a significant difference in the microstructure of the two material, with the as-cast material having a volume fraction of ferrite of about 59.4%, and large austenite grains segregated in

the ferritic matrix. While, for the heat-treated material, the fine austenite

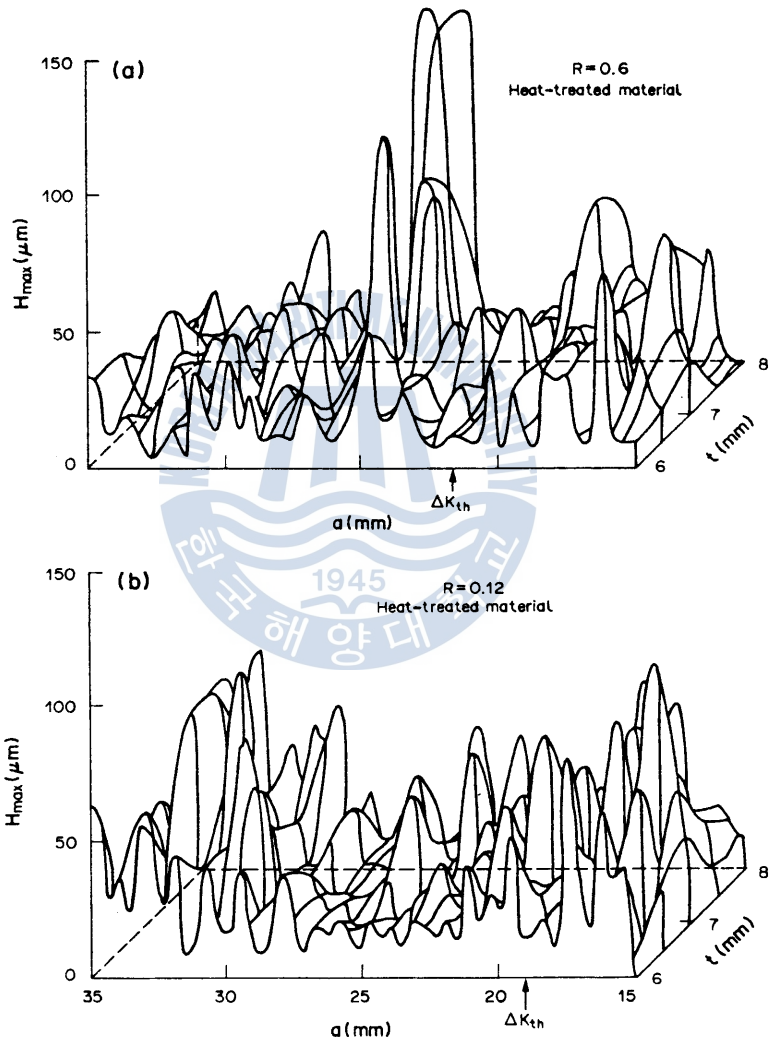

Fig. 6. Distribution of fracture surface roughness for a heat-treated specimen: (a) $R = 0.6$; (b) $R = 0.12$.

grains are uniformly distributed in the ferritic matrix. The fracture surface roughness should depend on the microstructural size which is confirmed by

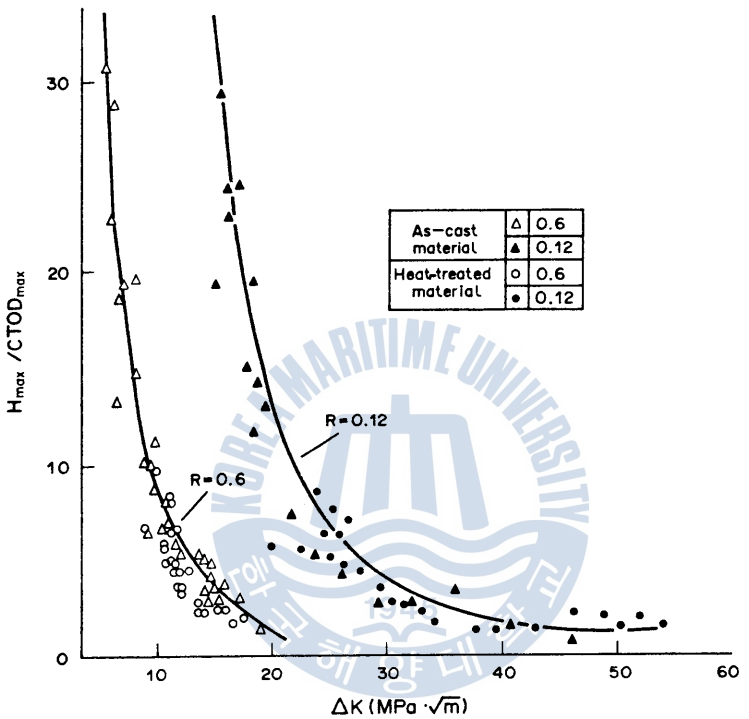

Fig. 7. Relationship between the ratio of surface roughness to CTOD$_{max}$ and ΔK.

the present data where the surface roughness is greater for the as-cast material than for the heat-treated material. The distribution of fracture surface roughness for a heat-treated specimen at $R = 0.12$ is shown in Fig.6(b). The fracture surface at the near threshold region is rougher for $R = 0.12$ than for $R = 0.6$. After ΔK_{th} was obtained crack growth was continued under constant load at a higher ΔK. Thus the fracture surface roughness becomes greater in this constant load crack growth region particularly for $R = 0.6$

In the near threshold region, the relative fracture roughness is expressed as the measured surface roughness divided by $CTOD_{\max}$, the maximum crack tip opening displacement, which is considered to be an important parameter [4]. Fig.7 shows the relationship between the ratio of surface roughness to $CTOD_{\max}$ and $\triangle K$. When the ratio of surface roughness to $CTOD_{\max}$is large, pronounced crack closure should occur. However the ratio of surface roughness to $CTOD_{\max}$ for the heat-treated specimen is almost the same as that for the as-cast specimen at both stress ratios. This differs from the variation in crack closure level reported above where it is greater for the heat-treated material than for the as-cast material. Park and Fine [3] have shown that the fraction of shear mode facets increases as the $\triangle K_{th}$ value is approached thus giving increasing surface roughness. Their result suggests that the mode II component significantly influences the crack closure behaviour at the near threshold region. As described region. As described in the fractographic results, there is a significant difference in the shear mode facets in the near threshold region of the two materials.

As shown in Figs 2 and 4. the near threshold crack growth rate for the heat-treated material is lower than that for the as-cast material at the same$\triangle K$ or $\triangle K_{eff}$. The data shown in Table 1 imply that the coarse austenite grain size of the as-cast material is responsible for the sharp drop in its Charpy absorbed energy although the change of tensile strength between heat-treated and as-cast material is relatively small. Also, because the solution treatment should promote partial transformation of α ferrite toγ austenite, the volume fraction of austenite should increase for the heat-treated specimen. The improvement of fracture toughness suggests that the increase in volume fraction of austenite and the fine austenite grain size, which resulted from solution treatment, contributes to an increase in the resistance to crack propagation in the near threshold region. Metastable austenite can be easily transformed to martensite by strain [5]. Such a transformation results in an

increase in the crack closure level thus improving the fatigue crack propagation resistance [5]. There is evidence of increasing crack closure level for the heat-treated specimen, as shown in Fig.3.

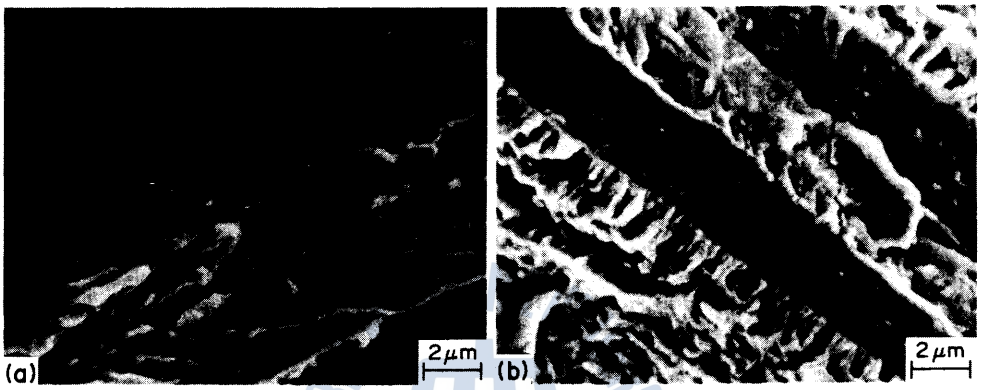

Fig. 8. Fracture morphology for the as-cast material: (a) $R = 0.6$, $\Delta K = 16$ MPa$\sqrt{\text{m}}$; (b) $R = 0.12$, $\Delta K = 11$ MPa$\sqrt{\text{m}}$.

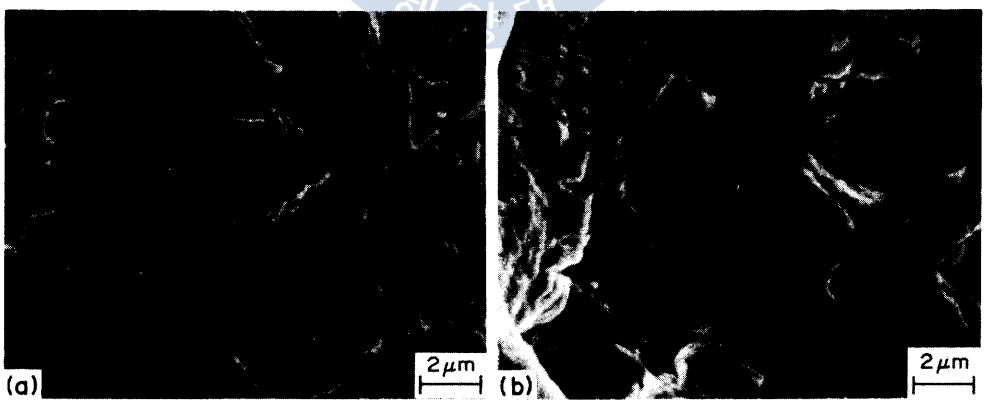

Fig. 9. Fracture morphology for the heat-treated material: (a) $R = 0.6$, $\Delta K = 8$ MPa$\sqrt{\text{m}}$; (b) $R = 0.12$, $\Delta K = 62$ MPa$\sqrt{\text{m}}$.

Figures 8 and 9 show the typical fracture morphology at $R = 0.12$ and 0.6 for the as-cast material and the heat-treated material, respectively. At high ΔK, striations are observed [see Fig. 9(b)]. As ΔK approaches ΔK_{th}, there is strong evidence for a microstructure-sensitive fatigue cracking process which exhibits a shear mode facet which depends on the microstructural size [see Figs 8(a), 8(b) and 9(a)]. In particular, the occurrence of a flat fracture appearance in the near threshold region suggests that the fatigue crack would arrest at austenite grains, and then grow along the interface of the grain. The size of the flat fracture appearance is greater for the as-cast than for the heat-treated material. At the near threshold region, the crack closure behaviour depends on not only the fracture surface roughness, but also the metallurgical parameters such as the microstructural and fracture feature dimensions.

Conclusions

(1) The crack growth rate decreased with decreasing stress ratio. When ΔK approached ΔK_{th}, the stress ratio strongly influenced the crack growth rate and ΔK_{th}.

(2) Analysis of the crack growth data using ΔK_{eff} showed that the effect of stress ratio could be explained but the effect of microstructure on crack growth could not.

(3) For the two-phase cast stainless steel, the roughness of the fracture surface was greater for the as-cast material than for the heat-treated material. However, the crack closure level was greater for the latter than for the former at a given stress ratio. The dependence of crack closure on the fracture surface roughness could be explained using the relative surface roughness. The crack opening and closure behaviour at the near threshold region is strongly dependent on the surface roughness and the strain-induced martensitic transformation.

References

1. P.C.Paris, R.J.Bucci, E.T.Wessel, W.G.Clark and T.R.Mager (1972) Extensive study of low fatigue crack growth rates in A533 and A508 steels. ASTM STP 573, pp.141–176.
2. R.J.Cooke, P.E.Irving, G.S.Booth and C.J.Beevers (1975) The slow fatigue crack growth and threshold behaviour of medium carbon alloy steel in air and vaccum. *Engng Fract. Mech.* 7, 69–77.
3. D.H.Park and M.E.Fine (1984) Origin of crack closure in the near-thresho-
   ld fatigue crack propagation of Fe and $Al-3\%Mg$. *In Fatiue Crack Growth Threshold Concepts* (Edited by D.Davidson and S.Suresh), pp. 145–161. Proceedings of AIME Conf., The Metallurgical Society, Philadelphia, Pa.
4. R.Murakami and Y.H.Kim (1989) On threshold characteristics and fatigue crack propagation behaviour of copper in high vacuum. *In Proc. Press. Vessel Tech. Nuclear Codes and Standards*, Seoul, pp.18/9–18/16.
5. R.Murakami, K.Akizono and K.Kusukawa (1986) Comparison of fatigue crack propagation under repeated impacts in stable and unstable stainless steels. *In Proc. Role of Fract. Mech. Modern Tech.* (Edited by G.C.Sih,H.Nisitani and T.Ishihara), pp.549–560. North-Holland, Fukuoaka.